

# Very Selective Volume Holograms: Manufacturing and Applications

**Nadya Reinhand**

*Russian Academy of Sciences, Institute of Mechanical Engineering Problems, V.O., Bolshoy pr., 61, St. Petersburg, 199178, Russia*

**Yuri Korzinin**

*Vavilov State Optical Institute, V. O., Birzhevaya, 12, St. Petersburg, 199034, Russia*

**Irina Semenova**

*A. F. Ioffe Physical Technical Institute, Russian Academy of Sciences, Polytechnicheskaya 26, St. Petersburg, 194021, Russia*

---

It is well known that transmissive and reflective type volume holograms have very high angular and spectral selectivity. Such highly selective holograms can find wide application in different fields, namely, three-dimensional imaging, diffraction optical elements, holographic storage, etc. The main problem in manufacturing thick holograms (of about a millimeter thickness) is in developing very thick photosensitive media, in which a grating can be recorded by illumination with an interference pattern. The analysis shows how different kinds of inhomogeneities and material shrinkage cause distortions in the reconstructed image and hologram selectivity properties. A review of the Russian materials (confirmed by experimental data) suitable for the recording of volume holograms is made.

Journal of Imaging Science and Technology 41: 241–248 (1997)

---

## Introduction

The term “volume” applied to holograms is associated with the ratio of hologram thickness to the period of the interference pattern recorded inside photosensitive material. If this factor is in excess of ten, the hologram exhibits volume properties that are well known.<sup>1</sup> The term “very thick”, we apply in cases when the thickness exceeds the period by a factor of about 3 orders. There are holograms with photosensitive material of millimeter thickness and high resolution; the regular interferometric pattern of about a thousand lines per millimeter can be recorded inside the material. Such holograms, both transmission and reflective types, possess spectral selectivity of about 0.1 nm and angular selectivity of about a milliradian. These characteristics are compatible with the ones given by regular optical devices, and therefore some of them can be replaced by the systems based on the usage of very thick holograms.

Usually the holographic photosensitive material of millimeter thickness is associated with photorefractive crystals, a variety of which were developed in recent years. Being the

dynamic media, they can find applications in holographic memory systems, in real-time interferometry, etc. However, the large range of applications requires stationary media.

Holographic imaging requires the application of holograms with high diffraction efficiency. Usually volume phase holograms whose theoretical efficiency is equal to 100% are used.<sup>1</sup> One of the drawbacks of holographic imaging is the necessity to record the hologram in coherent light. This limits the wide application of holography in everyday life. Recently a new scheme for hologram recording, the so-called reference-free selectogram,<sup>2</sup> was proposed. It permits both recording and reconstruction of a 3-D image in white light. It also has low sensitivity to the vibration of the elements of the recording scheme. To reach the good spatial resolution of the image, the photosensitive material should be of 1 to 3 mm thickness. The further development of very thick photosensitive materials can essentially contribute to the creation of a holographic camera of this type.

The variety of diffraction elements that use the high selectivity properties of thick holograms, namely filters, angular and spectral selectors, etc., can be designed based on very thick photosensitive materials. The angular selector proposed in Ref. 3 consists of two holograms, each of them representing a plane three-dimensional grating. The wave vectors of these holograms are perpendicular to each other. Each hologram of millimeter thickness performs the angular filtration of the incident beam with the milliradian bandwidth of selectivity contour. The construction of these two holograms permits the angular filtration of the incident beam into two dimensional perpendicular optical axes. The accuracy of this selection is equal to that of the traditional pinhole, while the system alignment is simpler and its sensitivity to different kinds of shifts is much lower. Another advantage of the holographic angular selector is in its possible application to powerful lasers where pinholes cannot work. Indeed, pinholes require light focusing, and thus the density of beam energy greatly increases at the focus to the point that it can destroy the filtering system. The holographic angular selector operates at the beam propagation angle, and therefore the laser beam energy threshold for these selectors is higher.

High spectral selectivity of thick holograms was used for the creation of a narrow-band selector<sup>4</sup> to be used in astronomy, laser optics, and optical location. The bandwidth of the angular selectivity contour obtained is 0.15 nm for the specimen recorded in photopolymer Reoxan of 1 mm thickness.

---

Original manuscript received November 10, 1996.

©1997, IS&T—The Society for Imaging Science and Technology

**TABLE I. Holographic Materials Suitable for Recording of Holograms of Millimeter Thickness**

		Sensitivity J/cm <sup>2</sup>	Thickness up to	Thermo-resistance	Drawbacks
1	Porous glass	depends on the media inside, usually 0.1-1	5 mm	up to 500°C	losses
2	Silver glass	1 – 10	100 mm	up to 500°C	recording at 300–350 nm
3	PDA photopolymer	~ 1	10 mm	up to 70°C	low thermoresistance
4	Reoxan	~ 1	10 mm	up to 70°C	low thermoresist, pre-exposure oxygen saturation
5	Gel-like dichromated gelatin	1 – 10	3 mm	up to 40°C	difficult to keep, low thermoresistance

It is known that the density of holographic storage depends greatly on the material thickness,<sup>5</sup> because the number of holograms that can be multiplexed at a single location depends on the hologram selectivity bandwidth that varies in inverse proportion to the hologram thickness. The recent successful experimental results on holographic storage in stationary media<sup>6</sup> are based on the usage of DuPont's HRF-150 photopolymer of 100  $\mu\text{m}$  thickness. By the application of the materials described next the storage density can be improved by order.

### Holographic Materials Suitable for the Recording of Very Thick Holograms

In this paper we limit our material review to the stationary media. All of them are developed in Russia (Table I.)

Porous materials<sup>7</sup> are the volume recording media based on the usage of a rigid silicate porous matrix, a silicate glass that is penetrated by the system of interconnecting pores. The photosensitive composition is introduced into the pores, but it covers only the surface (not the whole volume) of these pores. The other empty volume of pores forms a continuous capillary network providing the reagent penetration inside the specimen during the postexposure processing of holograms.

It should be mentioned that the capillary media based on porous materials are practically compressionless. Indeed, the photosensitive medium is connected rigidly with the matrix, and the characteristic sizes of cavities in which it is distributed are essentially less than the light wavelength. Therefore its deformation during the development process has a local character and does not distort the whole holographic structure.

The efforts of many researches show the possibility of introducing into the internal volume of porous materials a wide spectrum of photosensitive materials based either on organic compositions or on inorganic ones, namely: photopolymers, photochromic materials, silver halide media, photorefractive media, photostructuring compositions, and photoresist materials. Thus properties of resulting holographic materials may be widely varied by using different fillers.

Another light sensitive medium that can be used for the recording of very thick holograms is the so-called silver glass.<sup>8</sup> The photothermorefractive glasses consist of  $\text{SiO}_2\text{Al}_2\text{O}_3\text{ZnOLi}_2\text{O}(\text{Na}_2\text{O})$  doped with Ag and  $\text{CeO}_2$ . Under the action of Tungsten light illumination the photoinduced crystallization occurs inside this material. At first, radiation creates metal atoms in the glass, then the thermal treatment ( $T = 400^\circ\text{C}$ ) creates the metal colloids (color centers). These color centers work as the centers of nucleation during the next stage of the specimen processing: the treatment under higher temperature. The refractive index of the formed microcrystals,  $\text{Li}_2\text{O}$ ,  $\text{SiO}_2$ , or  $\text{NaF}$ , or  $\text{BaO}$ ,  $\text{SiO}_2$ , etc., differs from the refractive index of the glass, and therefore the structure inside the material is recorded.

Photopolymer holographic material with diffusive amplification (PDA)<sup>9</sup> is a medium consisting of polymethylmethacrylate (PMMA), including photochromic quinone molecules. The photoreconstruction reaction of the phenanthrenequinone in polymethylmethacrylate leads to the formation of phenanthrenic structures associated with polymers. As a result, at the stage of recording the two opposite phase gratings are produced, one of which is formed by variations of concentration of these phenanthrenic structures and the other by variations of concentration of free quinone molecules. During the postexposure processing (thermal treatment), the free quinone molecules are redistributed uniformly in the polymer matrix volume. This redistribution leads to a disappearance of one of the opposite phase gratings and, thus, to a considerable increase of the hologram diffraction efficiency.

Reoxan<sup>10</sup> is also based on the use of PMMA that serves as a matrix in which a photosensitive compound of anthracene structure is dispersed. Sensitization of the specimens is carried out by means of the polymer matrix saturation by oxygen inside the chamber with increased pressure. In the presence of the sensitizer, the photooxidizing reaction occurs inside the material caused by laser radiation. This reaction leads to the formation of photoinduced modulation of the material refractive index.

Dichromated gelatin (DCG) material is widely used for hologram and specklogram recording since the 1960s. Its modification, gel-like DCG,<sup>11</sup> is the moisture saturated layer; its thickness exceeds 10 to 15 times the thickness of the dry layer. This material is very useful for preliminary experiments due to its rather simple preparative procedure and cheapness. However, its keeping time is short even when the layer is protected from drying by a covering glass.

### Problems Associated with Photosensitive Materials

All photosensitive materials more or less possess a number of drawbacks, including, the change in average refractive index during the postexposure processing; the existence of shrinkage; and nonuniformity in depth of grating power, average refractive index, and shrinkage. The objective of this section is to attract the attention of researchers in the field of holographic materials to the consequences ensuing from these drawbacks. We estimate below the influence of these drawbacks on the quality of the reconstructed three-dimensional image as well as on the spectral and angular selectivity. It turns out that in many cases, even when the regular holographic materials of 10 to 100  $\mu\text{m}$  thickness are used, neglecting the effects associated with the above mentioned processes will cause essential errors in interpretation of experimental results.

**The Influence of the Average Refractive Index Changing and Shrinkage on the Reconstructed Image Quality.** The spatial frequency theory of three-dimensional holograms developed in Ref. 12 allows us to describe the image quality for the holograms of complex wave fields. It has been shown that for a three-dimensional

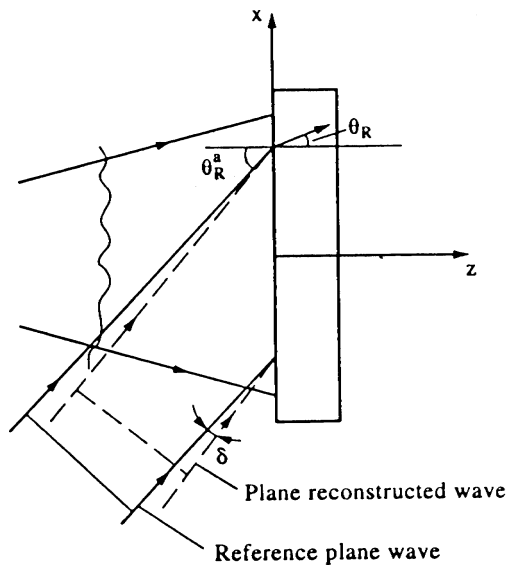


**Figure 1.** The problem of the reconstructed wave distortions by the hologram of complex wave field.

hologram recorded by a plane reference wave, the reconstructed image may be described by means of the optical transfer function of the hologram  $\Pi(\theta, \varphi)$ . This function makes the connection between angular spectra of the object  $S_o(\theta, \varphi)$  and reconstructed  $S_s(\theta, \varphi)$  waves:

$$S_s(\theta, \varphi) = \Pi(\theta, \varphi) S_o, \quad (1)$$

where  $\theta, \varphi$  are the azimuth and polar angles, respectively.

Consider the influence of the shrinkage and the average refractive index change on the transfer function for the case of the object wave with a continuous uniform angular power spectrum and normal incidence angle relative to the recording medium surface (Fig. 1). Consider that the reconstructing plane wave having the wavelength  $\lambda$  and incident angle  $\theta_R$  differs from the corresponding parameters of the reference wave by the values  $\Delta\lambda$  and  $\delta$ . We assume that after the recording stage, the hologram was subjected to uniform shrinkage  $\alpha$ , and its average refractive index was changed by  $\Delta n$ . Based on the results from Ref. 12 the transfer function may be expressed as follow:

$$\Pi(\theta, \varphi) = \Pi_3(\theta, \varphi) \exp(-i\beta T) \left\{ (1 + \alpha) \cos \theta - \alpha \cos \theta_R - \left[ 1 - (\sin \theta \cos \varphi / \beta)^2 \right]^{1/2} \right\}, \quad (2a)$$

where  $\beta = 2\pi n / \lambda$  and  $T$  is the hologram thickness.

$$\Pi_3(\theta, \varphi) = i \frac{A \cdot \exp[-iT(Q + \Delta Q) / 2]}{\cos \theta} \times \left\{ \frac{\sin \xi T}{\xi} \frac{\Gamma(\theta, \varphi) - Q}{Z^2(\theta, \varphi) - \xi^2} \left[ Z(\theta, \varphi) \frac{\sin \xi T}{\xi} - \sin Z(\theta, \varphi) T + i [\cos \xi T - \cos Z(\theta, \varphi) T] \right] \right\} \quad (2b)$$

$$\xi = \left[ \left( \frac{Q + \Delta Q}{2} \right)^2 + v^2 \right]^{1/2} \quad A = m\pi I_R / (\sqrt{\epsilon} \lambda \cos \theta_R),$$

$$\Delta Q = v\sqrt{P} \cos \theta_R,$$

Bragg mismatch for the corresponding angular component of reconstructing wave:

$$\Gamma(\theta, \varphi) = \Gamma_\delta(\theta, \varphi) + \Gamma_{\lambda, n}(\theta, \varphi) + \Gamma_\alpha(\theta, \varphi),$$

$$\Gamma_\delta(\theta, \varphi) = -\beta \delta (\sin \theta \cos \varphi \cos \theta_R - \cos \theta \sin \theta_R) / \cos \theta,$$

$$\Gamma_{\lambda, n}(\theta, \varphi) = \beta \left( \frac{\Delta n}{n} - \frac{\Delta \lambda}{\lambda} \right) (1 - \sin \theta \cos \varphi \sin \theta_R - \cos \theta \cos \theta_R) / \cos \theta,$$

$$\Gamma_\alpha(\theta, \varphi) = \beta \alpha (\cos \theta_R - \cos \theta);$$

where  $Q$  is the average Bragg mismatch,

$$Q = Q_\delta + Q_{\lambda, n} + Q_\alpha,$$

$$Q_\delta = \beta \delta \sin \theta_R,$$

$$Q_{\lambda, n} = -\beta \left( \frac{\Delta n}{n} - \frac{\Delta \lambda}{\lambda} \right) \left[ \cos \theta_R - \frac{tg(\Delta\theta / 2)}{\ln(1 + \sin \Delta\theta) - \ln(\cos \Delta\theta)} \right],$$

$$Q_\alpha = \beta \alpha \left[ \cos \theta_R - \frac{\Delta\theta / 2}{\ln(1 + \sin \Delta\theta) - \ln(\cos \Delta\theta)} \right],$$

$\Delta\theta$  is the angular divergence of the object beam.

$$Z(\theta, \varphi) = \Gamma(\theta, \varphi) - (Q + \Delta Q) / 2,$$

where  $m$  is the factor determined by the medium sensitivity and  $v$  is the hologram power, whose value is proportional to the exposure and determines its diffraction efficiency. (For  $v = \pi/4$ , the diffraction efficiency of the hologram is about 50%.)

Figures 2 and 3 represent the transfer function behavior for the change of the average refractive index of the hologram. The hologram of  $T = 1$  mm thickness is recorded with the object wave angular divergence  $\Delta\theta = 50$  deg and the incidence angle of the reference beam  $\theta_R = 30$  deg,  $v = \pi/4$ . The change of the refractive index is proposed to be  $\Delta n = 0.003$ . It has been taken into account for the calculation of the transfer function that the change of the average refractive index of hologram causes the change of the angle  $\theta_R$  by the value  $\delta = -tg(\theta_R) \Delta n / n$  due to the reconstructing beam refraction on the hologram boundary. The data shown in Figs. 2 and 3 and later in this section are related to the angular components of the object beam whose angular vectors are in the plane  $XOZ$  (Fig. 1), i.e., for  $\varphi = 0$  or  $\pi$ . The new azimuth angle  $\theta'$  is introduced that is positive for  $\varphi = 0$  ( $\theta' = \theta$ ) and negative for  $\varphi = \pi$  ( $\theta' = -\theta$ ). Figure 2 represents the dependence of  $|\Pi(\theta')|^2 / A^2$  on  $\theta'$  for the previously described case, and Fig. 3 represents the dependence of the transfer function phase  $\Phi$  on  $\theta'$ . As can be seen from the data, the change of the average refractive index leads to the essential nonuniformity of the transfer function inside the angular spectrum of the reconstructed wave. The attempt to compensate the nonuniformity in the transfer function amplitude by the change of the incidence angle of the reconstructed wave leads to some improvement of the uniformity of the transfer function amplitude (Fig. 2), but its phase is still very nonuniform (Fig. 3). The analysis of Eq. 2 shows that for the total compensation of the phase distortions, simultaneous change is required in the wavelength of the reconstructing beam by the value  $\Delta\lambda = \lambda \Delta n / n$ , and its incidence angle by the value  $\delta = tg(\theta_R) \Delta n / n$ . The latter compensates the  $\theta_R$  change caused by the wave refraction on the hologram boundary.

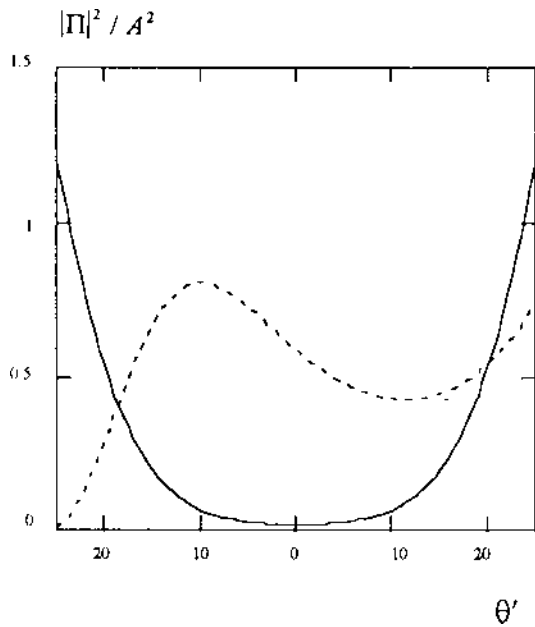


**Figure 2.** Square of modulus of the normalized transfer function of a 1-mm-thickness hologram subjected to uniform change of average refractive index of 0.3 % as it was being reconstructed by the reference wave (solid curve) and with a compensation of the amplitude distortions by the reconstructing wave incidence angle variation on  $\delta = 5 \times 10^{-4}$  rad (dotted curve).

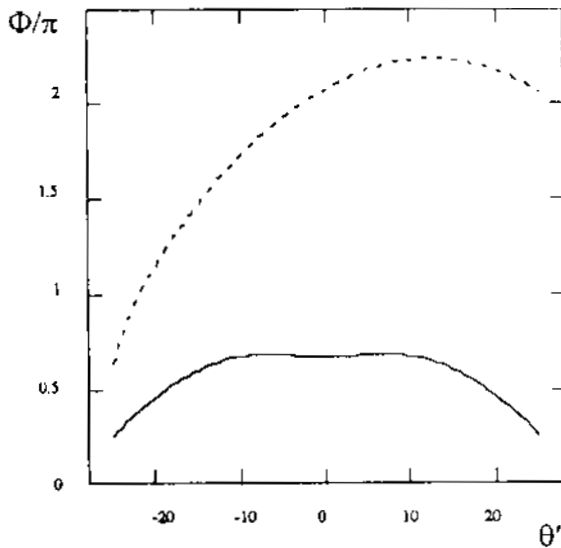


**Figure 3.** A phase of the transfer function of the hologram subjected to uniform change of refractive index and reconstructed under conditions corresponding to the data of Fig. 2.

The influence of the uniform shrinkage on the hologram transfer function is shown in Figs. 4 and 5. The same scheme parameters were used:  $\Delta\theta = 50$  deg,  $\theta_R = 30$  deg,  $T = 1$  mm, and  $\nu = \pi/4$ . The shrinkage value is proposed to be  $\alpha = 0.003$ . It can be seen from Figs. 4 and 5 that the uniform shrinkage of holograms leads to the essential distortions in the transfer function (solid curves). They cannot be compensated by the change of the incidence angle of the reconstructing beam (dotted curves). The analysis of Eq. 2 shows that the situation in this case ( $\alpha$ -type distortions) is different from the case described before ( $\Delta n$ -

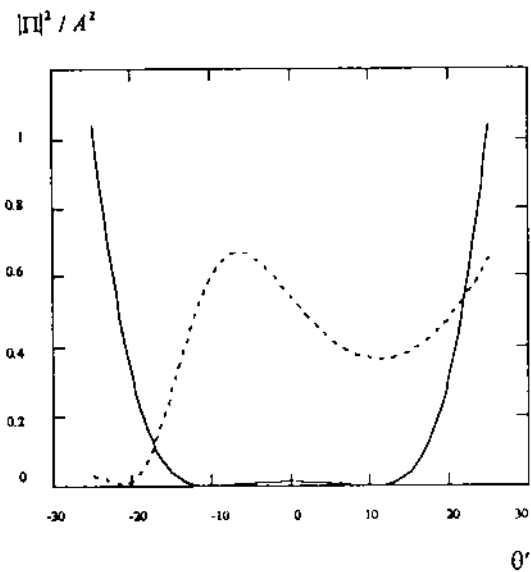


**Figure 4.** Square of modulus of the transfer function of a 1-mm-thickness hologram subjected to uniform shrinking of 0.3 % as it was being reconstructed by the reference wave (solid curve) and with a compensation of the amplitude distortions by the reconstructing wave incidence angle variation on  $\delta = 7 \times 10^{-4}$  rad (dotted curve).

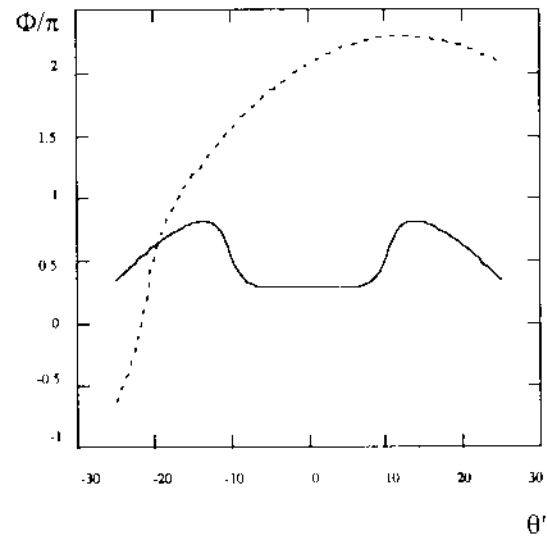


**Figure 5.** A phase of the transfer function of the hologram subjected to uniform shrinking and reconstructed under conditions corresponding to the data of Fig. 1.

type distortions). The transfer function distortions caused by the hologram shrinkage cannot be compensated even by simultaneous change in wavelength and incident angle of the reconstructing wave. This can be explained by the fact that the grating vectors of the hologram without shrinkage are located on an Ewald sphere, while for the hologram with uniform shrinkage they are located on the ellipsoid with the ratio of the axis lengths determined by the shrinkage value. This distortion of the sphere to the ellipsoid cannot be compensated by the changes in the reconstructing wave.

**Influence of Inhomogeneities on the Hologram Selectivity Properties.** Every photosensitive material suitable for the recording of volume holograms possesses different types of inhomogeneities: inhomogeneous distribution of the amplitude modulation of refractive index ( $n_1$ ), nonuniformity in depth of the average refractive index ( $n$ ), and inhomogeneity of the grating period in depth. These inhomogeneities are caused by the radiation absorption inside the material, its variable sensitivity, and the impact of the pre- and postexposure processings that lead to nonuniform shrinkage of the material.

Consider the most general case of the grating inhomogeneous in depth,<sup>13</sup> where  $n_1$ ,  $n$ , and  $Z$  components of the grating vector are changed  $K_Z(z) = K_Z(0) + \Delta K_Z(z)$ . (The  $OZ$  axis is directed inside the hologram perpendicular to its surface). Consider that the grating vector  $\vec{K}$ , wave vector of the incident wave  $\vec{\rho}$ , and the normal vector to the hologram surface are in one plane, and the electrical vector is perpendicular to this plane. In this case the field inside the hologram  $\Psi(\vec{r})$  can be described by the scalar wave equation:

$$\Delta\Psi = (\omega/c)^2 \varepsilon(\vec{r})\Psi(\vec{r}) = 0. \quad (3)$$

As previously mentioned, the hologram dielectric permeability  $\varepsilon(\vec{r})$  can be expressed as:

$$\varepsilon(\vec{r}) = \varepsilon_0 + \delta\varepsilon(z) + \varepsilon_1(z) \left[ \int_0^z K_Z(z) dz + K_X x \right], \quad (4)$$

where  $\delta\varepsilon(\vec{r}), \varepsilon_1(\vec{r}) \ll \varepsilon_0$ , and the scale of the average dielectric permeability of the grating  $[\delta\varepsilon(z)]$  as well as the scales of  $\varepsilon_1(z)$  and  $K_Z(z)$  are much larger than the wavelength and are compatible with the hologram thickness.

Further qualitative analysis is carried out in the approximation of single scattering of the incident wave on the periodic structure of the grating, and the wave propagation is described in the approximation of geometrical optics.<sup>14</sup> The latter is valid owing to the slow change of  $\delta\varepsilon(\vec{r}), \varepsilon_1(\vec{r})$  and  $K_Z(z)$ . Therefore the field inside the hologram volume is expressed in the form of superposition of incident  $R$  and diffracted  $S$  waves

$$\Psi(\vec{r}) = R(\vec{r}) + S(\vec{r}), \quad (5)$$

where the incident wave can be described<sup>14</sup> by the following expression:

$$\begin{aligned} R(\vec{r}) &= \frac{R_0 \sqrt{\rho_Z(0)}}{\sqrt{\rho_Z(z)}} \exp \left[ -i\rho_X x - i \int_0^z \rho_Z(z) dz \right] \\ \rho_Z(z) &= \sqrt{\beta^2(z) - \rho_X^2} \\ \beta(z) &= \frac{2\pi}{\lambda} \sqrt{\varepsilon_0 + \delta\varepsilon(z)} \end{aligned}, \quad (6a)$$

where  $R_0$  is the amplitude of the incident wave on the front surface of the hologram. The diffracted wave is expressed in the form:

$$\begin{aligned} S(\vec{r}) &= S(z) \exp \left[ -i\sigma_X x - i \int_0^z \sigma_Z(z) dz \right] \\ \sigma_X &= \rho_X + K_X \\ \sigma_Z &= \rho_Z + K_Z(z). \end{aligned} \quad (6b)$$

Substituting Eq. 6 into the wave Eq. 3, taking into account the approximations given, and neglecting non-Bragg orders of diffraction, we obtain the following expression for the complex amplitude of the diffracted wave:

$$S(z)' + i\Gamma(z)S(z) = -ik(z)R_0, \quad (7a)$$

where

$$\begin{aligned} \Gamma(z) &= \frac{\beta^2(z) - |\vec{\sigma}(z)|^2}{2\sigma_Z(z)}, \\ n_1(z) &= \frac{\varepsilon_1(z)}{2\sqrt{\varepsilon_0}}, \\ c_R &= \frac{\rho_{Z_0}}{\beta_0}, \\ \rho_{Z_0} &= \rho_Z(0), \\ k(z) &= \frac{\pi}{\lambda} n_1(z) \frac{1}{c_S}, \\ \beta_0 &= \beta(0), \\ c_S &= \frac{\sigma_{Z_0}}{\beta_0}, \\ \sigma_{Z_0} &= \sigma_Z(0) \end{aligned} \quad (7b)$$

and the Bragg mismatch  $\Gamma(z)$  can be expressed in an explicit form:

$$\Gamma(z) = \Gamma_0 + \beta_0 \frac{dn(z)}{n_0} \left( \frac{1}{c_S} - \frac{1}{c_R} \right) - \frac{\Delta K_Z(z)}{c_S^2}, \quad (8a)$$

$$n_0 = \sqrt{\varepsilon_0}, \quad dn(z) = \frac{\delta\varepsilon(z)}{2\sqrt{\varepsilon_0}}. \quad (8b)$$

In Eq. 6a,  $\Gamma_0 = [\beta_0^2 - |\sigma(0)|^2]/2\sigma_{Z_0}$ , the Bragg mismatch on the front surface of the hologram is described by Kogelnik's formulas,<sup>15</sup> and the second and third terms are the additional mismatch caused by the inhomogeneities of the average refractive index  $[dn(z)]$  and the grating period  $[\Delta K_Z(z)]$ .

The solution of Eq. 7a is well known,<sup>16</sup> and under the zero boundary conditions on the front surface of the hologram the amplitude of the diffracted wave on the back surface is

$$S(T) = -i \exp(-i\Gamma_0 T) R_0 \int_0^T f(z) \exp(i\Gamma_0 z) dz, \quad (9a)$$

$$f(z) = k(z) \exp \left\{ -i \int_0^T \beta_0 \frac{dn(z')}{n_0} \left( \frac{1}{c_S} - \frac{1}{c_R} \right) - \frac{\Delta K_Z(z')}{c_S^2} \right\} dz'. \quad (9b)$$

It can be seen from Eqs. 9a and 9b that the amplitude of the diffracted wave is equal to a Fourier transform of the distribution of the grating power  $[k(z)]$  multiplied by some phase function whose character is determined by the behavior of the average refractive index  $(dn)$  and  $Z$  component of the grating vector  $(\Delta K_Z)$ . It should be pointed out that according to Ref. 15, the Bragg mismatch  $\Gamma_0$  is the linear function of the angular deviation  $(\delta)$  and wavelength

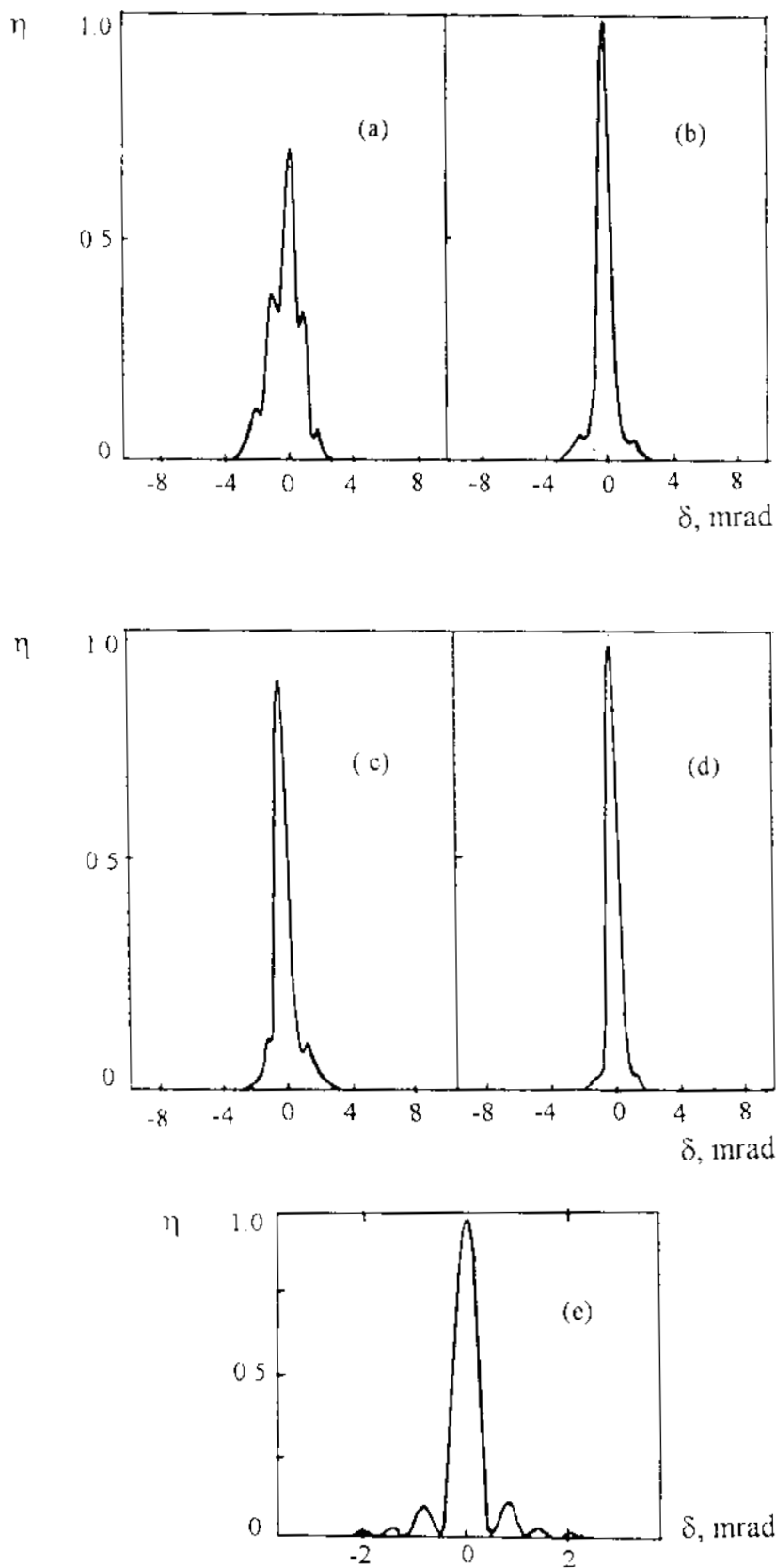


**Figure 6.** Angular selectivity contours for the holograms recorded: (a) in porous glass with the thickness of  $T = 1.8$  mm and spatial frequency of  $\xi = 2200$   $\text{mm}^{-1}$ , (b) in porous glass,  $T = 1.2$  mm,  $\xi = 900$   $\text{mm}^{-1}$ ; (c) and (d) in photopolymer with diffusive amplification (PDA)  $T = 2$  mm,  $\xi = 900$   $\text{mm}^{-1}$ ; and (e) calculated selectivity contour for the plane grating, where  $\delta$  is the deviation of the incident angle from the Bragg angle.

deviation ( $\Delta\lambda$ ) of the reconstruction conditions from the Bragg ones. Therefore in our approximation the contours of the grating angular and spectral selectivity are the square modulus of the Fourier transform of the function  $f(z)$  within the accuracy of scale coefficients, i.e.,

$$\eta(\Gamma_0) \sim \hat{f}(\Gamma_0) \hat{f}^*(\Gamma_0), \quad (10)$$

where  $\eta(\Gamma_0)$  is the diffraction efficiency and  $\Lambda$  indicates Fourier transform.

Figure 6 represents the experimentally measured angular selectivity contours for the holograms in porous glass [Figs. 6(a) and 6(b)], photopolymer PDA, [Figs. 6(c) and 6(d)], and the calculated contour for the uniform grating [Figs. 6(e)]. It should be pointed out that most of the gratings recorded in porous glass and some gratings recorded in PDA have asymmetric contours of angular selectivity. According to Eqs. 10 and 9b, this asymmetry cannot be associated with the inhomogeneity of the grating power in depth because  $k(z)$  is a real function and its Fourier transform is Hermitian  $\hat{k}(\Gamma_0) = \hat{k}^*(-\Gamma_0)$ . Therefore the diffraction efficiency is a symmetric function of  $\Gamma_0$ :

$$\eta(\Gamma_0) = \eta(-\Gamma_0) \sim \hat{k}(\Gamma_0) = \hat{k}^*(-\Gamma_0) = \hat{k}(-\Gamma_0) \hat{k}(-\Gamma_0) \quad (11)$$

for  $dn$ , and  $\Delta K_z = 0$ .

This permits us to draw the conclusion that the resulting holograms possess inhomogeneity in depth of the average refractive index or  $z$  component of the grating vector. The first type of inhomogeneity is natural for the holograms in porous glass. It is the result of the transport processes during the etching stage<sup>17</sup> and during the filling of the free space inside the pores by the photosensitive medium. However, for the symmetric grating ( $c_s = c_r$ ,  $K_z = 0$ ) according to Eq. 9b the influence of  $n$  and  $K_z$  inhomogeneities is equal to zero. The measured asymmetry of the selectivity contours for the holograms in porous glass is caused by some errors in the orientation of the recording material ( $c_s \neq c_r$ ). The asymmetry of the contour for the holograms in PDA is also caused by the deviation from the symmetric scheme and probably by the nonuniform deformation in depth of the samples during the postexposure processing, i.e., by the appearance of the variable component  $K_z$ .

It is interesting to point out that the phase of function  $f$  decreases with the increase of the wavelength of the incident wave. This must lead to the reduction of the contour asymmetry in the long wave spectral range. However, simultaneously with the increase of wavelength the Bragg angle of reconstruction increases and the difference  $(1/c_r - 1/c_s)$  can increase faster than the wavelength  $\lambda$  growth (Fig. 7). The latter leads to the enhancement of the influence of phase inhomogeneities on the selectivity contour in the long wave spectral regime.

The analysis of Eq. 9 shows that the value of side maxima of the selectivity contours is determined mainly by the inhomogeneity of the grating power  $[k(z)]$ . Side maxima grow up when the drop in the  $k(z)$  function occurs in the middle of the grating, and these maxima weaken when the grating power decreases from the grating center to hologram surfaces.<sup>18</sup> The fall in the sensitivity in the center of the porous recording material of 1.8 mm thickness [Fig. 6(a)] is caused by incomplete etching of the glass during the process of the porous sample preparing. Special methods for introduction of the photosensitive material into the porous glass and formation of holograms in PDA<sup>19</sup> permit compen-

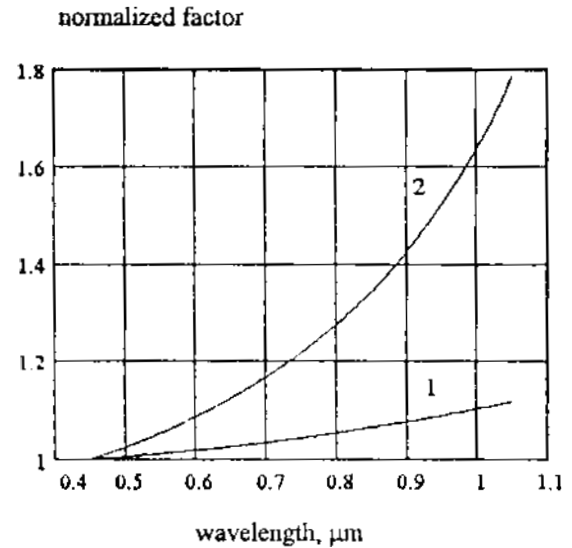


**Figure 7.** Coefficient  $(1/C_R - 1/C_S)/\lambda$  normalized to its value at  $\lambda = 0.450 \mu\text{m}$  via wavelength  $\lambda$ : (1)  $\xi = 1000 \text{ mm}^{-1}$  and (2)  $\xi = 2000 \text{ mm}^{-1}$ ; [the inclination angle of isophase surfaces is  $(-1) \text{ deg}$ ].

sation of the distribution of the grating power in the material depth and, therefore, suppression of the side maxima in selectivity contours [Figs. 6(b) and 6(d)].

## Conclusions

Very selective stationary (nondynamic) holograms of millimeter thickness can find applications in different fields, namely in three-dimensional imaging and in systems for holographic storage, as well as different kinds of diffraction optical elements in laser optics, astronomy, etc. The holographic materials suitable for the recording of holograms of millimeter thickness is reviewed briefly in this paper. The main problem associated with the manufacturing of such holograms is in preparing the photosensitive materials with minimal shrinkage and inhomogeneities. The analysis has been carried out on the influence on the image quality and selectivity properties of the following parameters: the change of average refractive index during the postexposure development; shrinkage; and nonuniformity in depth of grating power, average refractive index, and shrinkage. It was shown that the small changes in the average refractive index and shrinkage (of about 0.003) lead to extremely large distortions in the reconstructed image both in phase and amplitude that leads to losses in the reconstructed image resolution. The inhomogeneities in depth of grating power, average refractive index, and shrinkage affect mainly the behavior of the selectivity contour and can lead to its broadening and asymmetry. The latter is important to take into account, for example, for the calculation of the information capacity of holographic memory systems based on volume holograms. All the effects mentioned above reduce with the decrease of the hologram thickness, but even for ordinary holographic materials they are observed.  $\blacktriangle$

## References

1. R. J. Collier, C. B. Burckhardt, and L. H. Lin, *Optical Holography*, Academic Press, New York and London, 1971, p. 689.
2. Y. N. Denisuyk, "Window effect of 3-D deep hologram as a base of 3-D imaging by means of a selectogram (Reference-free selectogram)," *Practical Holography IX*, S. A. Benton, Ed., *Proc. SPIE* **2406**, 65 (1995).

3. Y. L. Korzinin, N. O. Reinhand, and I. V. Semenova, et al., "Two-dimensional holographic nonspatial filter," *Proc. SPIE* **2688**, 109 (1996).
4. V. I. Sukhanov, Y. V. Ascheulov, A. E. Petnikov, and G. I. Lashkov, "3D hologram in Reoksan as a narrow-band spectral selector," *Pis'ma Zh. Tekh. Fiz.* **10**, 925 (1984).
5. H.-Y. S. Li and D. Psaltis, "Three-dimensional holographic disks," *Appl. Opt.* **33**, 3764 (1994).
6. G. Barbastathis, A. Pu, and D. Psaltis, "Shift multiplexed holographic 3D disk," *Proc. SPIE* **2689**, 220 (1996).
7. S. A. Kuchinsky, V. I. Sukhanov, and M. V. Khazova, "Principles of hologram formation in capillary composites," *Optics Spectr.* **72**, 716 (1992).
8. S. A. Kuchinsky, N. V. Nikonov, E. I. Panysheva, V. V. Savvin, and I. V. Tumanova, "Properties of volume phase holograms in polychromatic glasses," *Soviet J. Optics Spectr.* **70**, 757 (1991).
9. A. V. Veniaminov, V. F. Goncharov, and A. P. Popov, "Hologram amplification due to diffusion destruction of opposite phase structures," *Optics Spectr.*, **70**, 864 (1991).
10. G. I. Lashkov, and V. I. Sukhanov, "The use of dispersion photorefractive caused by the processes with triplet states for recording phase three-dimensional holograms," *Optika i Spektroskopija* **44**, 1008 (1978).
11. Y. N. Denisjuk, N. M. Ganzharli, and I. A. Maurer, "Recording of deep volume holograms in gel-like layers of dichromated gelatin," *Lett. J. Tech. Phys.* **21**, 51 (1995).
12. Y. L. Korzinin and V. I. Sukhanov, "Spatial-frequency version theory of three-dimensional holograms," *Opt. Laser Tech.* **28**, 311 (1996).
13. Y. L. Korzinin, V. L. Alekseev, A. M. Kursakova, et al., "Holographic spatial-frequency filter for laser radiation," *J. Opt. Phys.* (in press).
14. L. M. Brehovskikh, *Waves in layer media*, USSR Academy of Sciences, Moscow, 1957, p. 502 (in Russian).
15. H. Kogelnik, "Coupled wave theory for thick hologram gratings," *Bell Syst. Tech. J.* **48**, 2909 (1969).
16. V. I. Smirnov, *High Mathematics*, Vol. 2, Nauka, Moscow, 1974, p. 655. (in Russian).
17. T. M. Burkat, G. K. Kostyuk, and E. B. Yakovlev, Structural anisotropy and double beam refraction in the plates of porous glass," *Glass Physics Chem.* **17**, 781 (1991).
18. A. P. Yakimovich, "Apodization of selective response of volume holograms," *Opt. Spectrosc.* **53**, 1066 (1982).
19. A. P. Popov, A. V. Veniaminov, and Y. N. Sedunov, "Photochemical and diffusion apodization of thick phase holograms," *Opt. Comm.* **110**, 18 (1994).